Multilayer Quasi-Linear Viscoelastic Characterization of Porcine Aorta Using Nanoindentation

Ali Hemmasizadeh[1], Soroush Assari[1], Kurosh Darvish[1] and Michael Autieri[2]
[1]Department of Mechanical Engineering, Temple University, Philadelphia, PA
[2]Department of Physiology, School of Medicine, Temple University, Philadelphia, PA

ABSTRACT

In a wide range of biomechanical modeling of aorta from traumatic injury to stent grafts, the arterial wall has been considered as a single homogeneous layer vessel, ignoring the fact that arteries are composed of distinct anatomical layers with different mechanical characteristics. In this study, using a custom-made nanoindentation technique, changes in the mechanical properties of porcine thoracic aorta wall in the radial direction were characterized using a quasi-linear viscoelastic model. Two layers of equal thickness were mechanically distinguishable in descending aorta based on the radial variations in the instantaneous Young's modulus E and reduced relaxation function G(t). Overall, comparison of E and $G\infty$ of the outer half (70.27±2.47 kPa and 0.35±0.01) versus the inner half (60.32±1.65 kPa and 0.33±0.01) revealed that the outer half was stiffer and showed less relaxation. The results were used to explain local mechanisms of deformation, force transmission, tear propagation and failure in arteries.

INTRODUCTION

Arterial mechanical properties have received increasing attention in the past few decades due to their vast effect on predicting cardiovascular diseases and injuries. On one side of this effort, researchers investigated the mechanobiological behavior of healthy and diseased arteries in the physiological range to obtain better characterization of cardiovascular diseases such as atherosclerosis, which afflicts about 795,000 Americans every year (Roger *et al.*, 2011), and on the other side they developed mathematical models to predict large deformations and injuries such as Traumatic Aortic Rupture (TAR), which is one of the leading causes of fatality in motor vehicle crashes (Richens *et al.*, 2003). For this purpose diverse methodologies have been utilized, among them are static and dynamic uniaxial and biaxial tests (Mohan and Melvin 1983; Bass *et al.*, 2001), inflation tests (Schulze *et al.* 2002), and indentation tests (Ebenstein and Pruitt 2004).

In most of the previous studies the arterial wall was considered as a single homogeneous layer vessel ignoring the fact that arteries are composed of three anatomically distinct layers. Tunica intima is the innermost layer consisting of a single layer of endothelial cells that line the lumen. In healthy young human this layer is very thin and does not have a significant contribution to the wall mechanical behavior but its thickness and stiffness generally increases with age (Holzapfel and Gasser 2000). Such changes in intima with age have not been observed in animals. Tunica media is the middle layer consisting mainly of elastin lamellae, collagen, and smooth muscle cells (SMC). Elastin lamellae and the interlamellar elastin fibers form a cage-like structure that surrounds the SMC (O'Connell *et al.* 2008). Media is responsible for the elastic recoil that maintains blood pressure during diastole. Tunica adventitia is the outermost layer consisting of mostly longitudinally running collagen fibers, thin elastic fibers, and fibroblasts. The adventitia's main mechanical function is to prevent excessive dilatation and permanent deformation (Fung 1996).

The mechanical characteristics of separated arterial layers have been studied by a few investigators. In these studies, two or three layers were distinguished based on histological investigations and the layers were separated mechanically by cutting along the anatomical boundaries. Holzapfel *et al.* (2005) investigated three layers of human coronary arteries with nonatherosclerotic intimal thickening using cyclic quasi-static uniaxial tension tests superimposed on 5% prestretch and found significantly different anisotropic mechanical properties for these layers. The reported ratios of adventitia, media and intima thicknesses to total wall thickness were 0.4, 0.36, and 0.27 respectively. Based on their average experimental results, the Young's modulus in the low loading domain (at which the noncollagenous matrix material is mainly active) was lower for media compared to adventitia (approximately 20 kPa versus 200 kPa). Teng *et al.* (2009) quantified the ultimate strength of human atherosclerotic carotid arteries by direct mechanical testing of media and adventitia. They identified the adventitia and media visually with equal thickness and found that adventitia was stiffer than media. In the axial direction, the adventitia ultimate strength (1996±867 kPa) was significantly higher than media (519±720 kPa) while their stretch ratios at failure (1.54±0.23 and 1.40±0.18 respectively) were not significantly different.

Most test methods used for characterizing the mechanical properties of arteries are dealing with the macroscopic properties of vessels. Recently nanoindentation techniques have been used to describe the local material properties of various tissues including bone (Rho *et al.* 1997), teeth (Habelitz *et al.* 2001), cartilage (Pierce *et al.* 2010) and vascular tissues (Ebenstein and Pruitt 2004; Matsumoto *et al.* 2004; Levental *et al.* 2010). Ebenstein *et al.* (2004) used conospherical tips for nanoindentation of internal surface of porcine aorta. They applied a trapezoidal load control profile and calculated the reduced modulus in the range of 700-800 kPa based on the method of Oliver and Pharr (1992) which considered an elastic material in unloading. Matsumoto *et al.* (2004) developed a scanning micro indentation setup, a scaled-up version of the atomic force microscope (AFM), and determined the Young's modulus distribution of the lamellar unit (separated media) of porcine aorta in the axial and circumferential directions in the range of 50-180 kPa where the lower and higher values corresponded to the smooth muscle-rich layer (SML) and elastic lamina (EL) respectively. They reported no significant difference between the sections with different directions.

In this study, using a custom-made nanoindentation technique, local changes of the mechanical properties of porcine thoracic aorta wall in the axial direction were characterized. The results are summarized as a multilayer viscoelastic material model which can be used to investigate local mechanisms of aorta deformation, force transmission, tear propagation and failure.

MATERIALS AND METHODS

Seven fresh porcine aorta specimens were obtained from a local slaughterhouse (Hatfield Quality Meats, Hatfield, PA). Each specimen was submerged in physiologic Phosphate Buffered Solution (PBS) immediately post-mortem and stored in an ice filled cooler while transported to the Laboratory. Specimens were cleaned from the surrounding tissues and thirty four 8-10 mm long cylindrical samples were excised from two locations. Group *A* (n=20 at three sections) were extracted inferior to the first intercostal arteries and Group *B* (n=14 at two sections) at 40 mm inferior to Group *A* (Fig. 1).

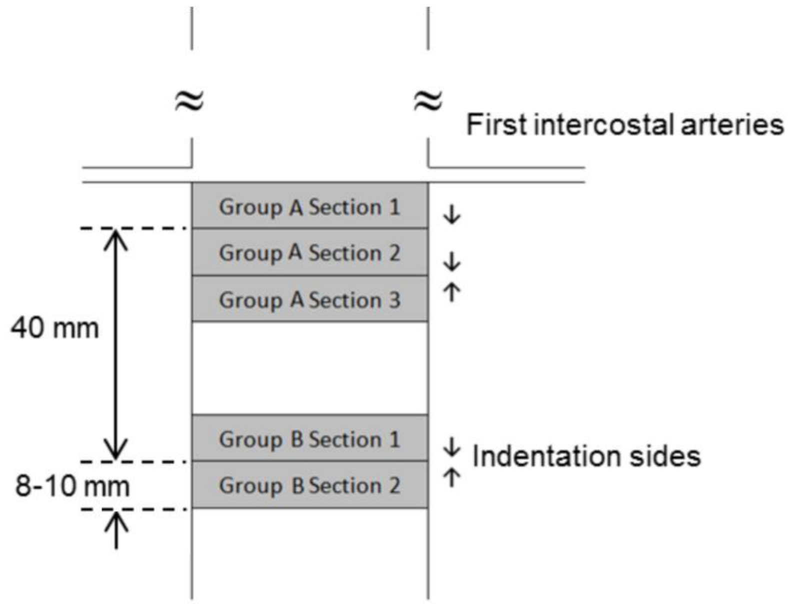

Fig. 1. Schematic of locations of different groups and their indentation test directions.

A custom-made test setup was designed to perform nanoindentation tests (Fig. 2), consisting of a Z-axis nano-positioner with resolution of 0.2 nm and 100 μm range of motion (Nano-Z100, MCL,WI) combined with a horizontal piezo micro-positioner (M-663.4 PX, PI, MA). A conical indenter (XPT, Agilent Technologies, CA, 55° tip angle, 10 μm tip rounding radius) was attached to a force transducer (Aurora Scientific, Ontario, Canada, Model 406A) with resolution of 0.1μN. The setup was equipped with a horizontally positioned 300x Stereo Microscope (Olympus SZX7) for contact visualization and the whole setup was mounted on an active vibration isolation table (TMC 63-533 Peabody, MA).

Soft tissues material properties are sensitive to hydration (Solanes *et al.* 2004). Preliminary results showed that force and consequently elastic modulus of aorta increased when the tissue dried. Therefore, to avoid dehydration, ring-shaped samples were placed in a 15 mm height aluminum container and were immersed in PBS to their top surface. Since the density of aorta is more than PBS, samples stayed stationary and no adhesive was used. As the indenter tip was lowered to make contact with the sample top surface, it first became in contact with a thin layer of PBS and resulted in a small tensile load due to the liquid surface tension. The tip was lowered further to the point when the tensile load started to decrease, which was considered to be the initial point of contact with the tissue (Cao *et al.* 2005).

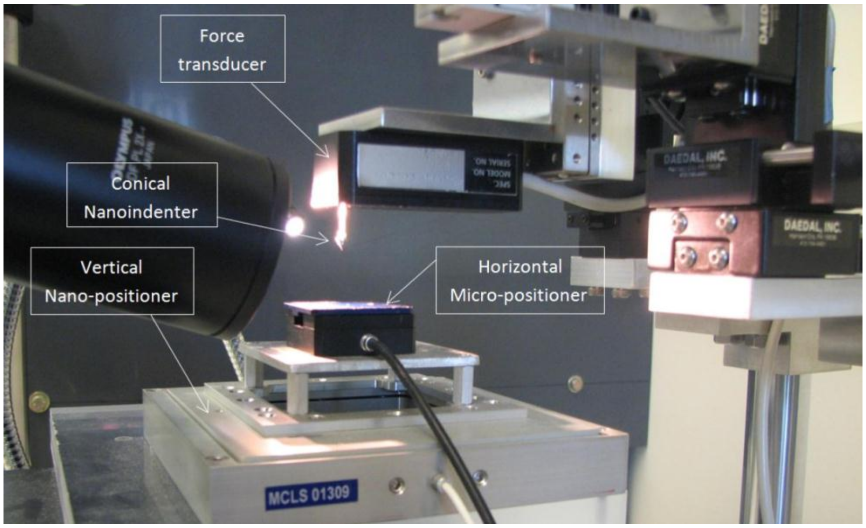

Fig. 2. Experimental setup for nanoindentation.

The indentation tests were performed in the longitudinal direction at various points along the thickness of aorta (Fig. 3). The indentation site was chosen at 90° counter-clockwise with respect to intercostal arteries to minimize the variability due to circumferential location. For each sample, the indenter tip was aligned to the outermost layer of aorta and the first point of indentation was 100 μm inward from this point. Successive indentation tests were performed toward the innermost layer with distances of 100 μm or 200 μm between points. The average wall thickness was 1.76±0.05 mm and depending on local wall thickness 6 to 13 points were tested on each sample. The distance of the indentation points from the innermost layer was normalized (r) based on the wall thickness, where r=0 represented the innermost layer and r=1 the outmost layer. Samples were moved upward toward the indenter with a ramp and hold displacement with 40 μm indentation depth, 10 ms ramp time and 30 s hold time. The force and displacement data were collected at 5 kHz. All indentation tests were conducted in less than eight hours post-mortem.

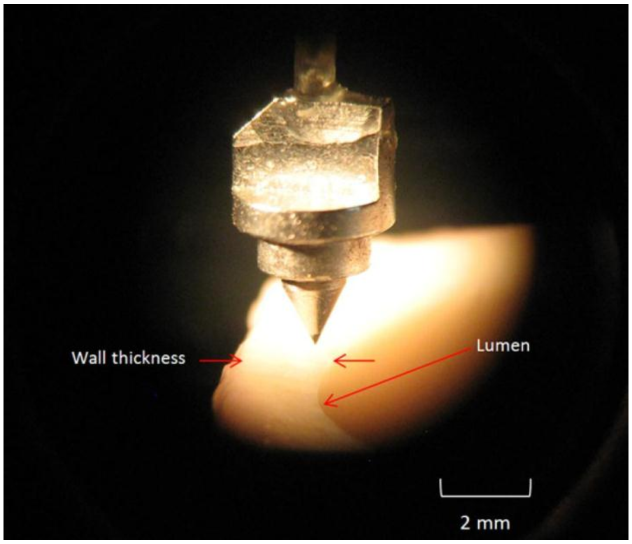

Fig. 3. Conical tip used for nanoindentation along aorta wall thickness.

FORMULATIONS

The mechanical behavior of the vessel in axial indentation was characterized assuming the material to be locally homogeneous, isotropic and linearly viscoelastic. The force history of the indenter in loading $P(t)$ was written in terms of the indentation depth $h(t)$ using a quasi-linear viscoelastic (QLV) model (Fung 1996):

$$P(t) = \int_0^t G(t-\tau) \frac{\partial P^e(h)}{\partial h} \frac{\partial h}{\partial \tau} d\tau \tag{1}$$

in which $P^e(h)$ is the instantaneous elastic force that can generally be a nonlinear function of h. $G(t)$ is the reduced relaxation function which was assumed to be a Prony series:

$$G(t) = G_\infty + \sum_{i=1}^{4} G_i \exp(-\beta_i t) \tag{2}$$

in which G_i and β_i represent the relaxation amplitudes and decay rates respectively. According to the ramp and relaxation times, four decay rates were chosen to capture the decays that occurred during the tests (β_1 = 0.1, β_2 = 1, β_3 = 10, and β_4 = 100 s^{-1}). P^e was selected based on the total elastic load necessary to cause a penetration h for a conical indenter which can be written as (Sneddon 1965):

$$P^e = \frac{2E \cot(\beta)}{\pi(1-\nu)} h^2 \tag{3}$$

where β is the cone angle with respect to the horizontal axis (β=62.5°), E is the instantaneous Young's modulus, and v is the Poisson's ratio which was assumed to be 0.5 (incompressible) for fresh aorta due to its high water content.

RESULTS

From nanoindentation tests, the viscoelastic material properties (Equations. 2 and 3) were obtained by fitting the model to experimental force history curves using a direct integration

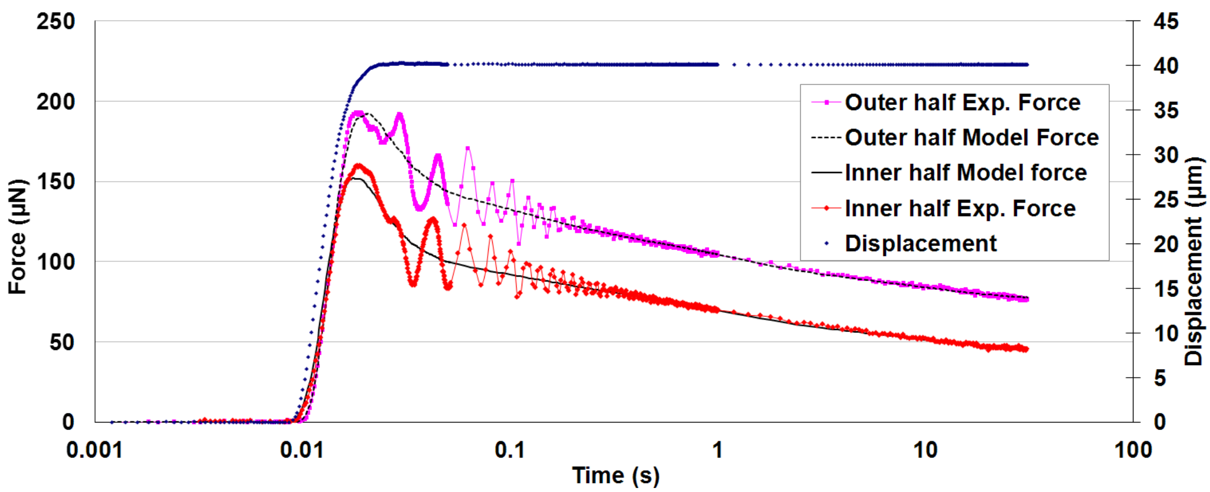

Fig. 4. Force and displacement history curves from typical indentation tests inner and outer halves of aorta thickness.

technique for the viscoelastic response to a general input (Simo and Hughes 1998) and the method of least squares. The relaxation data was resampled (0-0.05 s at 5 kHz, 0.05-1 s at 250 Hz, 1-30 s at 5 Hz) to give approximately equal weights to different time scales. Representative curve fit results for the inner half of wall thickness ($0 < r \leq 0.5$) and the outer half ($0.5 < r \leq 1.0$) are shown in Fig. 4 which shows the experimental forces including the peak forces were matched adequately (An overall R^2 values of 0.9 or greater were achieved). The transient vibration observed in the response was due to sample natural frequency (dependent on sample geometry and material properties) which did not affect the viscoelastic characterization. A representative force-displacement curve (corresponding to the ramp region) is shown in Fig. 5 which demonstrates good agreement between the QLV model and experimental data. This Figure also verifies the quadratic form of the elastic function (Equation 3) and that the effect of relaxation was negligible for small displacements due to the short applied ramp time.

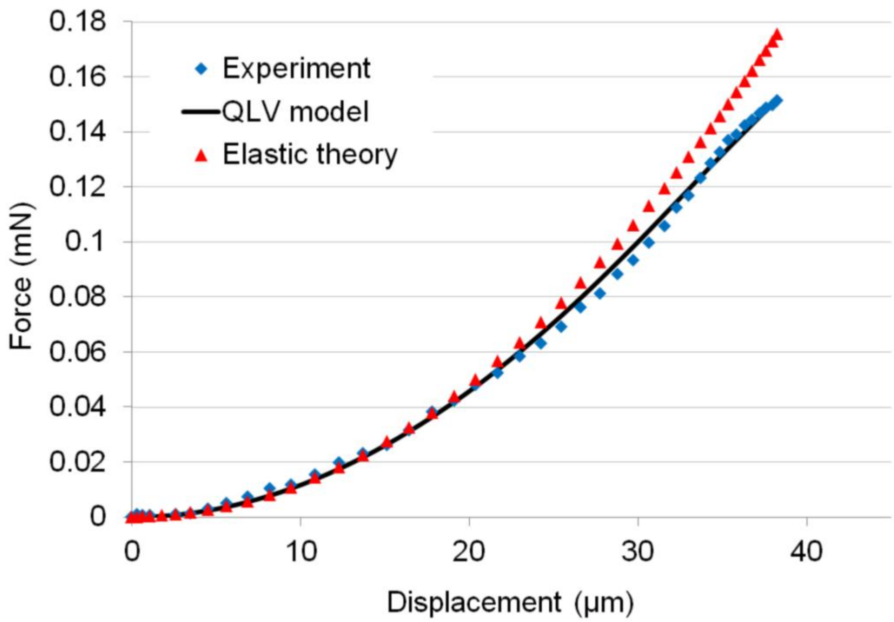

Fig. 5. Representative indentation force-displacement curves for the elastic theory, experimental data and QLV model.

To achieve a better understanding of the trend of distribution of the material properties within the aorta wall, the results of Groups *A* and *B* were divided into 10 regions based on *r*. The variation of *E* with respect to *r* is shown in Fig. 6a which demonstrates that the outer half was generally stiffer than the inner half. The grouping of material properties in to inner and outer halves (Fig. 6b) was verified by applying hierarchical cluster analysis (JMP SAS, Version 8, Cary, NC) in which the regions data were combined in several steps into clusters whose values were closer to each other relative to those of other clusters based on Ward's minimum variance. Additionally, paired *t*-test was conducted between *E* in the inner half and outer half of all samples (Table 1) which confirmed a significant difference ($p<0.001$) between these regions. Therefore, it can be concluded that $r = 0.5$ acted as a cut-off for the inhomogeneity of *E* in the radial direction. Paired *t*-tests on G_i showed that G_∞ and G_1 were significantly higher in the outer

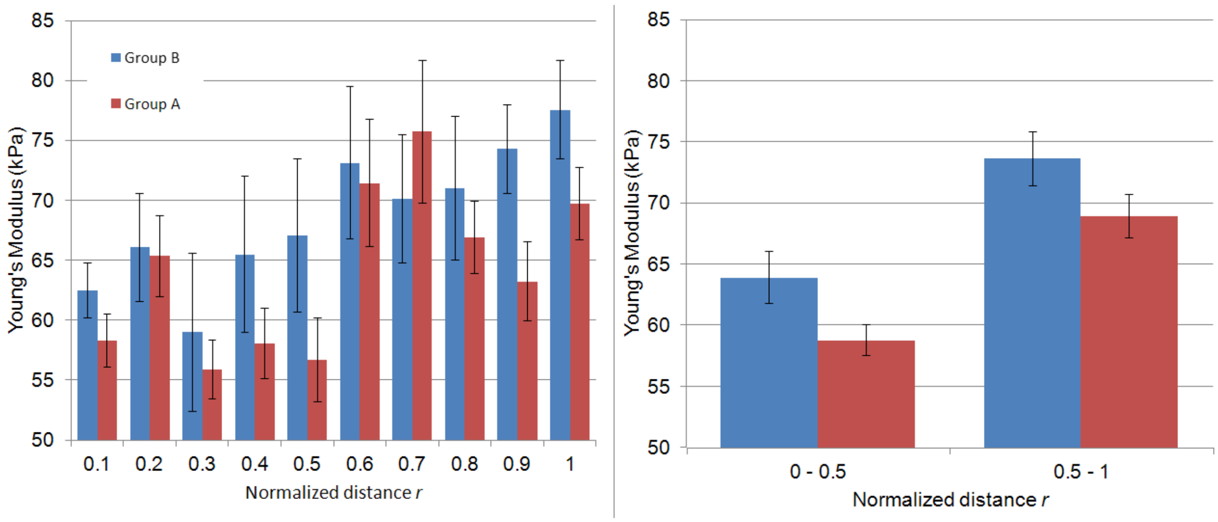

Fig. 6. a) Distribution of E in 10 regions along the aorta wall thickness. b) Average values of E for inner and outer halves.

half region and G_4 was significantly lower (Table 1). This means that the outer half was generally more elastic than the inner half.

Table 1. The average values of E and G_i for inner half and outer half regions and their standard errors and p values for paired two-tail t-tests.

	E	G_∞	G_1	G_2	G_3	G_4
Inner half	60.32±1.65	0.33±0.01	0.07±0.01	0.11±0.01	0.13±0.01	0.36±0.01
Outer half	70.27±2.47	0.35±0.01	0.09±0.01	0.10±0.01	0.13±0.01	0.34±0.02
p-value	0.001	0.006	0.043	0.353	0.247	0.032

Comparison of sections 2 of Groups A and B with paired t-test was used to evaluate the heterogeneity of material properties due to 40 mm longitudinal distance. The results (Table 2) showed that E was significantly higher (p=0.03) in Group B but G_i were not significantly different. In other words, the material was heterogeneous with respect E but homogeneous with respect to $G(t)$ in the longitudinal direction.

Table 2. The average values of E and G_i in two sections that are 40 mm apart and their standard errors and p values for paired two-tail t-tests.

	E	G_∞	G_1	G_2	G_3	G_4
Group B Section 2	64.60±4.76	0.35±0.02	0.12±0.02	0.10±0.01	0.13±0.02	0.29±0.03
Group C Section 2	69.32±3.40	0.36±0.02	0.12±0.02	0.12±0.01	0.17±0.02	0.23±0.03
p-value	0.03	0.28	0.38	0.04	0.14	0.13

DISCUSSION

An indentation technique was developed to study local variability of the viscoelastic behavior of aorta wall with respect to the radial distance. The test setup enabled reaching 40 μm spatial resolution and 10 regions were characterized on the aorta wall thickness. It was determined that below the first intercostal arteries, two larger regions with equal thickness were mechanically distinguishable with significantly different values of instantaneous Young's modulus (E) and reduced relaxation function ($G(t)$). The thicknesses of media and adventitia layers are reported to be almost the same (Holzapfel and Gasser 2000; Teng *et al.* 2009) and for the young specimens used in this study, it was expected that the intima layer was significantly thinner that the other two layers (Holzapfel and Gasser 2000). Therefore, it may be concluded that the inner and outer halves of aorta approximately coincide with the media and adventitia layers respectively.

Characterization of the material behavior was based on the QLV theory applied to the force data obtained during loading in a displacement-control setup. The force time histories (Fig. 4) and force displacement curves (Fig. 5) verified the applicability of the QLV model (Equations 1 to 3). In elastic and elastic-plastic materials, often the unloading force-displacement curve in a force-control setup is used for material characterization to eliminate the effect of friction during loading (e.g., Oliver and Pharr, 1992). However, in viscoelastic materials, due to creep (delay in displacement response), the unloading force-displacement curve would overestimate the material stiffness. This may explain the relatively high values of Young's modulus (700-800 kPa) determined by Ebenstein *et al.* (2004) for porcine aorta.

The viscoelastic behavior of aortic tissue was characterized by the values of relaxation amplitudes G_i. In particular, G_∞ showed that the steady state Young's modulus was on average 34% of the instantaneous Young's modulus. G_∞, G_1, and G_4 for inner half and outer half were significantly different from each other, which implied that aorta wall long-term and short-term damping mechanisms were also inhomogeneous. Overall, the outer layer showed less damping, which may be attributed to the layers infrastructure. The damping mechanism in media, in addition to the movement of interstitial fluid within the solid phase cage-like microstructure, can be attributed to smooth muscle cells (SMC) that constitute about 24% of this layer (O'Connell *et al.* 2008). SMC in non-active state, without the presence of a vasoconstrictor, show significant viscoelasticity (Fung 1996). Therefore, lack of SMC in adventitia makes it effectively more elastic.

The knowledge of the material properties of aortic wall is fundamental to the understanding of aorta failure mechanisms and how a local tear propagates through the aortic wall. Many instances of partial aortic rupture occur (about 10 to 20%) in which the outermost layer of aorta does not rupture and the chance of survival of the patient is significantly increased (Fattori *et al.* 1994). Considering aorta as a pressure vessel, the inner layers are exposed to higher stress levels than the outer layers (Lai et al., 2010). Mohan and Melvin (1983) showed that the failure of aorta is strain based with approximately 50% and 60% ultimate strain for quasi-static and dynamic (80 s^{-1} strain rate) stretch tests respectively. Moreover, Holzapfel *et al.* (2005) reported that the ultimate stretches are similar for separated aorta tissue layers. The results of this study revealed that, in descending aorta, the inner layer is more compliant than the outer one. Therefore, it can be concluded that, based on only pressure loading, the inner layer would sustain higher strains and would be more vulnerable to failure. In other words, failure in aorta would propagate from inner layers toward the outer layers. This conclusion is in agreement with several previous experimental studies on blunt carotid injuries Cogbil *et al.* (1994), Fabian *et al.* (1996), Punjabi *et al.* (1997), Cohuet et al. (2001), and the tensile experiments on aorta by Teng *et al.* (2009).

Surface detection is a challenge in nanoindentation of soft materials and the changes in the adhesion force curve are generally used to determine the point of contact (Cao *et al.* 2005, Kaufman 2009, Ebenstein, 2011). In this study, the adhesion force between the PBS layer and indenter tip was maximum 6 µN tension and the initial decrease in this force (after about 1-2 µm displacement) was considered as the point of contact which is in agreement with Cao *et al.* (2005). This force was much smaller than the maximum indentation force (about 170 µN) and was considered negligible in the analysis.

It should be noted that Equation (3) used for the elastic solution of conical indenters is derived for infinitesimal deformations and assumes the material to be locally isotropic and homogeneous. In terms of homogeneity, this study is limited by the resolution of the indentation site (40 µm). This resolution, however, was sufficient to achieve the conclusions regarding the material properties of inner and outer halves in the radial direction. The comparison of experimental force-displacement curves with the theoretical model (Fig. 5) demonstrated that the application of Equation (3) in the present study was valid. At higher indentation depths the experimental force is slightly less than the theoretical values, which is due to viscoelastic relaxation that occurred during the 10 ms ramp time. This relatively small ramp time made the calculated elastic Young's modulus to be closer to the true instantaneous Young's modulus of the material (Fung 1996) which requires a step change in displacement. However, this ramp time resulted in transient vibration after the peak force due to the sample inertia. It was confirmed that the frequency of this vibration (approximately 60 Hz) coincided with the first natural frequency of samples in the longitudinal direction (Gladwell *et al.*, 1972). It was assumed that the effect of this transient vibration was negligible in the conclusions of this study as the viscoelastic model passes approximately through the local average forces (Fig. 4). Although, aorta in vivo is in tension, it should be noted that Eq. 3 implies that the material behavior is the same in tension and compression as long as the deformations are small.

ACKNOWLEDGEMENTS

The support for this work was provided partially by the NHLBI under Grant Number K25 HL086512-03 and Grant Number R21 HL088159-02.

REFERENCES

Amabile, P., Collart, F., Gariboldi, V., Rollet, G., Bartoli, J.M., P. Piquet, 2004. Surgical versus endovascular treatment of traumatic thoracic aortic rupture. J. Vasc. Surg. 40, 873-879.

Bass, C.R., Darvish, K., Bush, B., Crandall, J.R., Srinivasan, S.C., Tribble, C., Fiser S., Tourret, L., Evans, J.C., Patrie J., Wang C., 2001. Material properties for modeling traumatic aortic rupture. Stapp. Car Crash J. 45, 143-60.

Cao, Y., Yang D., Soboyejoy. W., 2005. Nanoindentation method for determining the initial contact and adhesion characteristics of soft polydimethylsiloxane. J. Mater. Res. 20, 2004-2011.

Cogbill, T.H., Moore, E.E., Meissner, M., *et al.*, 1994. The spectrum of blunt injury to the carotid artery: a multicenter perspective. J. Trauma. 37, 473-479.

Cohuet, G., Challande, P., Osborne-Pellegrin, M., Arribas, S.M., Dominiczak, A., Louis, H., Laurent, S., Lacolley, P., 2001. Mechanical strength of the isolated carotid artery in SHR. Hypertension. 38, 1167-1171.

Ebenstein, D. M., 2011. Nano-JKR force curve method overcomes challenges of surface detection and adhesion for nanoindentation of a compliant polymer in air and water. J. Mater. Res. 26, 1026-1035.

Ebenstein, D.M., Pruitt, L.A., 2004. Nanoindentation of soft hydrated materials for application to vascular tissues. J. Biomed. Mater. Res. 69A, 222–232.

Ebenstein, D.M., Pruitt, L.A., 2006. Nanoindentation of biological materials. Nanotoday 1, 26-33.

Fabian, T.C., Patton, J.H., Croce, M.A., Minard, G., Kudsk, K.A., Pritchard, F.E., 1996. Blunt carotid artery injury: importance of early diagnosis and anticoagulant therapy. Ann. Surg. 223, 513-525.

Fattori, R., Celletti, F., Bertaccini, P., Galli, R., Pacini, D., Pierangeli, A., Gavelli, G., 1996. Delayed Surgery of Traumatic Aortic Rupture. Circulation. 94, 2865-2870.

Fischer-Cripps, A.C, 2011. Nanoindentation, 3rd ed., Springer.

Fung, Y.C., 1996. Biomechanics Mechanical Properties of Living Tissues. Springer.

Gladwell, G.M.L., Tahbildar, U.C., 1972. Finite element analysis of the axisymmetric vibrations of cylinders. J. Sound Vibration. 22(2), 143-157.

Holzapfel, G.A., Gasser, T.C., 2000. A new constitutive framework for arterial wall mechanics and a comparative study of material models. J. Elasticity 61, 1–48.

Holzapfel, G.A., Sommer, G., Gasser, C.T., Regitnig, P., 2005. Determination of layer-specific mechanical properties of human coronary arteries with nonatherosclerotic intimal thickening and related constitutive modeling. AM. J. PHYSIOL-HEART C. 289, H2048–H2058.

Kaufman, J. D., 2009. Surface detection errors cause overestimation of the modulus in nanoindentation on soft materials. J Mech Behav Biomed Mater. 2, 312-317.

Lai, W.M, Rubin, D., Krempl, E., 2010. Introduction to Continuum Mechanics, 4th ed., Elsevier.

Lally, C., Reid, A.J., Prendergast, P.J., 2004. Elastic behavior of porcine coronary artery tissue under uniaxial and equibiaxial tension. Annals of Biomedical Engineering, 32, 1355-1364.

Levental, I., Levental, K.R., Klein, E.A., Assoian, R., Miller, R.T., Wells, R.G., Janmey, P.A., 2010. A simple indentation device for measuring micrometer-scale tissue stiffness. Journal of Physics: Condens. Matter 22, 194120-28.

Matsumoto, T., Goto T., Furukawa T., Sato M., 2004. Residual stress and strain in the lamellar unit of the porcine aorta: Experiment and analysis. J. Biomech. 37, 807-815.

Mohan, D., Melvin, J.W., 1983. Failure properties of passive human aortic tissue. I-uniaxial tension tests. J.Biomech. 16, 31-37.

O'Connell, M.K., Murthy, S., Phan, S., Xu, C., Buchanan, J., Spilker, R., Dalman, R.L., Zarins, C.K., Denk, W., Taylor, C.A., 2008. The three-dimensional micro- and nanostructure of the aortic medial lamellar unit measured using 3D confocal and electron microscopy imaging. Matrix Biol. 27, 171-181.

Oliver, W.C., Pharr, G.M., 1992. An improved technique for determining hardness and elastic modulus using load and displacement sensing indentation experiments. J. Mater. Res. 7, 1564-1583.

Pierce, D.M., Trobin, W., Raya, J.G., Trattnig, S., Bischof, H., Glaser, C., Holzapfel, G.A., 2010. DT-MRI Based Computation of Collagen Fiber Deformation in Human Articular Cartilage: A Feasibility Study. Ann. Biomed. Eng. 38, 2447–63.

Punjabi, A.P., Plaisier, B.R., Haug, R.H., Malangoni, M.A., 1997. Diagnosis and management of blunt carotid artery injury in oral and maxillofacial surgery. J. Oral Maxillofac Surg. 55, 1388-1395.

Qi, H.J., Joyce, K., Boyce, M.C., 2003. Durometer hardness and the stress-strain behavior of elastomeric materials. Rubber Chem. Technol. 72, 419-435.

Richens, D., Kotidis, K., Neale, M., Oakley, C., Fails, A., 2003. Rupture of the aorta following road traffic accidents in the United Kingdom 1992–1999. The results of the co-operative crash injury study. Eur. J. Cardio-thoracic 23, 143–148.

Roger, V.R., Go, A.S., Lloyd-Jones, D.M., Adams, R.J., *et al.*, 2011. Heart disease and stroke statistics--2011 update : A report from the American Heart Association. Circulation. 123, e18-e209.

Schulze Bauer, C.A., Regitnig, P., Holzapfel, G.A., 2002. Mechanics of the human femoral adventitia including the high-pressure response. Am. J. Physiol. Heart Circ. Physiol. 282, H2427-40.

Simo, J.C., Hughes T.J.R., 1998. Computational Inelasticity, first ed. Springer.

Sneddon, I.N., 1965. The relation between load and penetration in the axisymmetric boussinesq problem for a punch of arbitrary profile. Int. J. Eng. Sci. 3, 47-57.

Solanes, N., Rigol, M., Castella, M., Khabiri, E., Ramirez, J., Segales, J., Roque, M., Agusti, E., Perez-Villa, F., Roig, E., Pomar, J.L., Sanz, G., Heras. M., 2004. Cryopreservation alters antigenicity of allografts in a porcine model of transplant vasculopathy. Transplant. P. 36, 3288-3294.

Teng, Z., Tang, D., Zheng, J., Woodard, P.K., Hoffman, A.H., 2009. An experimental study on the ultimate strength of the adventitia and media of human atherosclerotic carotid arteries in circumferential and axial directions. J. Biomech. 42, 2535–2539.

Vande Geest, J.P., Sacks, M.S., Vorp, D.A., 2004. Age dependency of the biaxial biomechanical behavior of human abdominal aorta. Journal of Biomechanical Engineering, 126, 815-822.

Virues Delgadillo, J.O., Delorme, S., El-Ayoubi, R., Diraddo, R., Hatzikirakos, S.G., 2010. Effect of Freezing on the Biaxial Mechanical Properties of Arterial Samples. J Biomedical Science and Engineering 3,645-652.